Supporting information for

Metal-free Energy Storage Systems: Combining Batteries with Capacitors based on Methylene Blue Functionalized Graphene Cathode

Yadi Zhang[a,b], Yufeng An[a], Langyuan Wu[a], Heng Chen[a], Zihan Li[a], Hui Dou[a],

Vignesh Murugadoss[b,c,d], Jincheng Fan[b,e] Xiaogang Zhang[a*], Xianmin Mai,[f,*] Zhanhu Guo[b*]

a. Jiangsu Key Laboratory of Electrochemical Energy Storage Technologies, College of Material Science and Engineering, Nanjing University of Aeronautics and Astronautics, Nanjing 210016, China. E-mail: azhangxg@nuaa.edu.cn

b. Integrated Composites Laboratory, Department of Chemical and Biomolecular Engineering, The University of Tennessee, Knoxville, TN 37996, USA. E-mail: zguo10@utk.edu.

c. Key Laboratory of Materials Processing and Mold (Zhengzhou University), Ministry of Education, National Engineering Research Center for Advanced Polymer Processing Technology, Zhengzhou University, Zhengzhou, China

d. School of Materials Science and Engineering, North University of China, Taiyuan 030051, China

e. College of Materials Science and Engineering, Changsha University of Science and Technology, Changsha 410114, China

f School of Urban Planning and Architecture, Southwest Minzu University, Chengdu 610041, China E-mail: maixianmin@foxmail.com

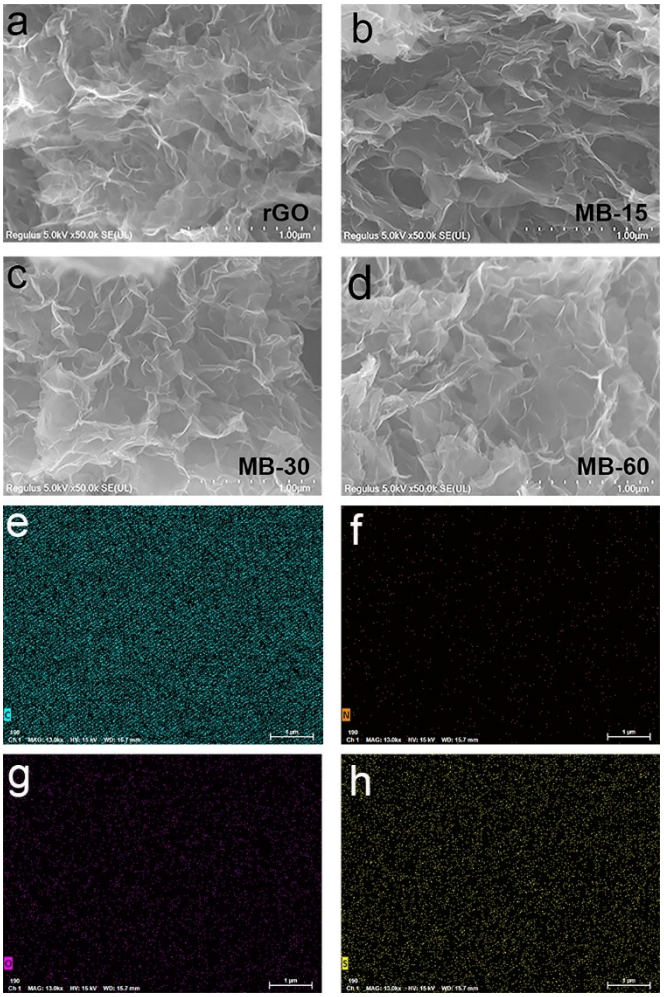

Fig. S1 SEM images of (a) rGO, (b) MB-15, (c) MB-30, and (d) MB-60, and element-mapping of (e) C, (f) N, (g) O and (h) S.

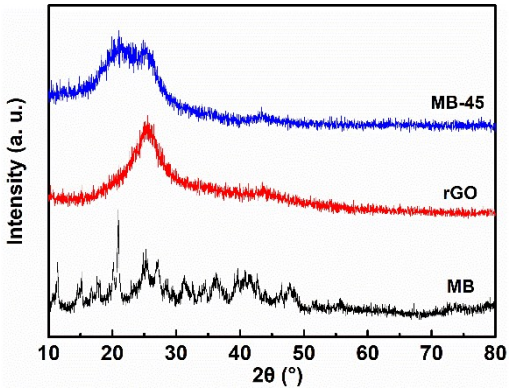

Fig. S2 XRD patterns of (a) rGO, MB and MB-45.

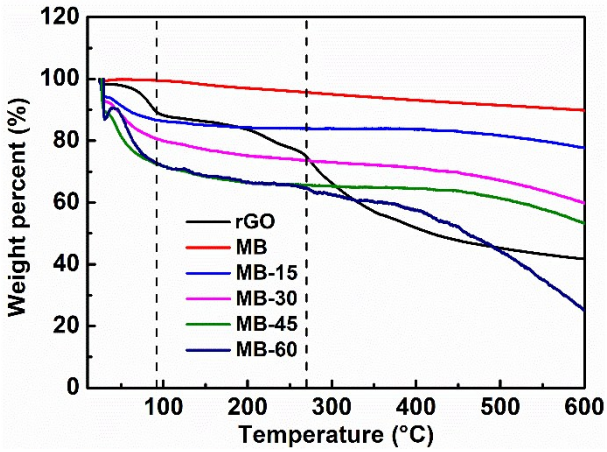

Fig. S3 TG analysis of rGO and MB-X samples.

We also investigated the thermal properties of the rGO and all MB-X samples in air (Fig. S3). The slight weight loss of rGO mainly results from the labile oxygen-containing groups. As for MB, there are two main mass loss processes. One is between 30 and 100 ºC that is ascribed to the removal of adsorbed water molecules, and the other in the range from 100 to 250 °C belongs to the decomposition of MB. In comparison, the MB contents in the MB-X samples are 14.5%, 27.5%, 34.6% and 37.8%, respectively. The differences between theoretical contents and practical contents are attributed to the adsorption area of rGO.

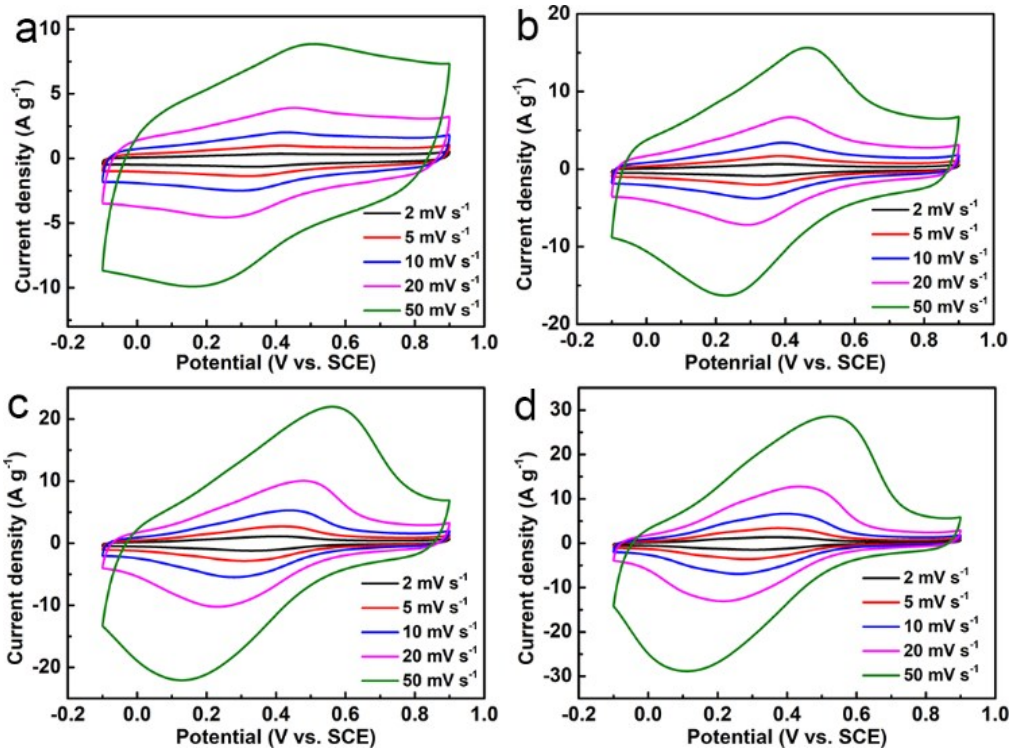

Fig. S4 CV curves at different scan rates of (a) rGO, (b) MB-15, (c) MB-30 and (d) MB-60.

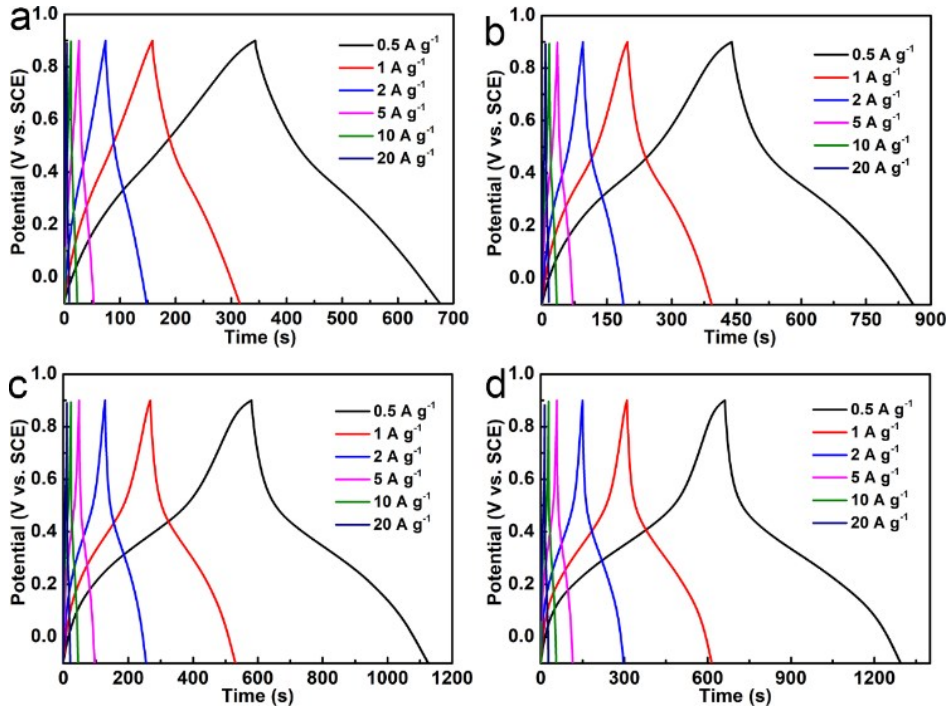

Fig. S5 GCD curves at various current densities of (a) rGO, (b) MB-15, (c) MB-30 and (d) MB-60.

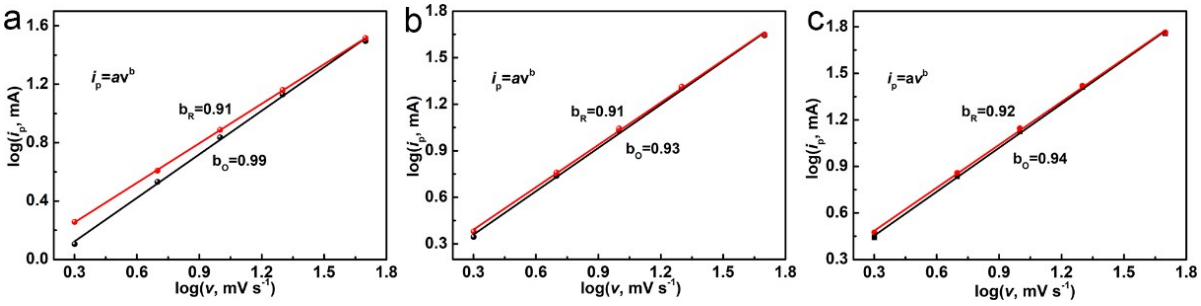

Fig. S6 Relationships between log*i* and log*v* based on peak currents of (a) MB-15, (b) MB-30 and (c) MB-60.

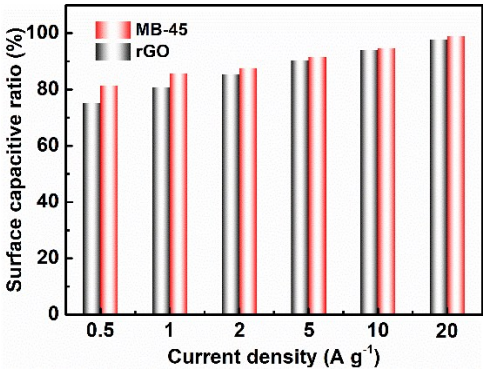

Fig. S7 Surface capacitive ratio as different current densities of rGO and MB-45.

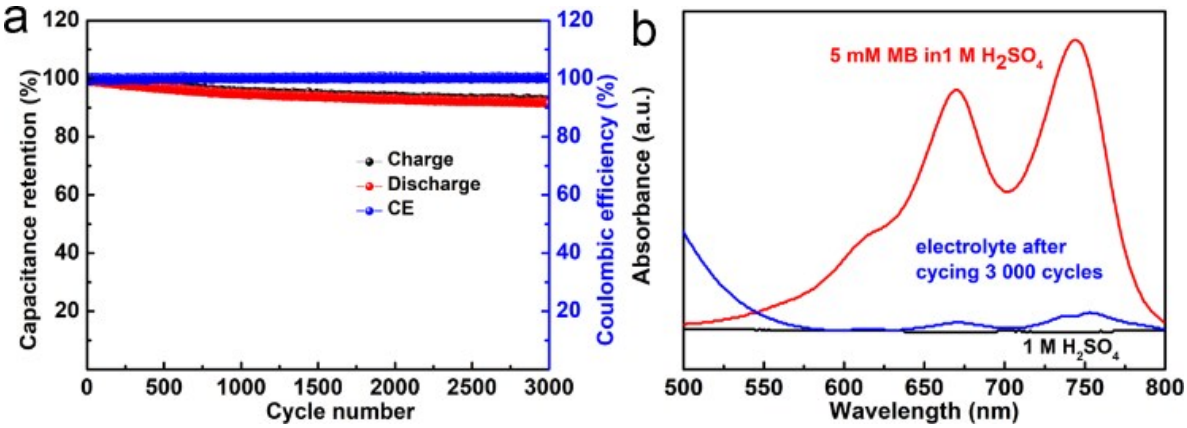

Fig. S8 (a) Cycle performance and Coulombic efficiency of MB-45, (b) UV spectra of 5 mM MB in l M H_2SO_4 and electrolyte after cycling 3 000 cycles.

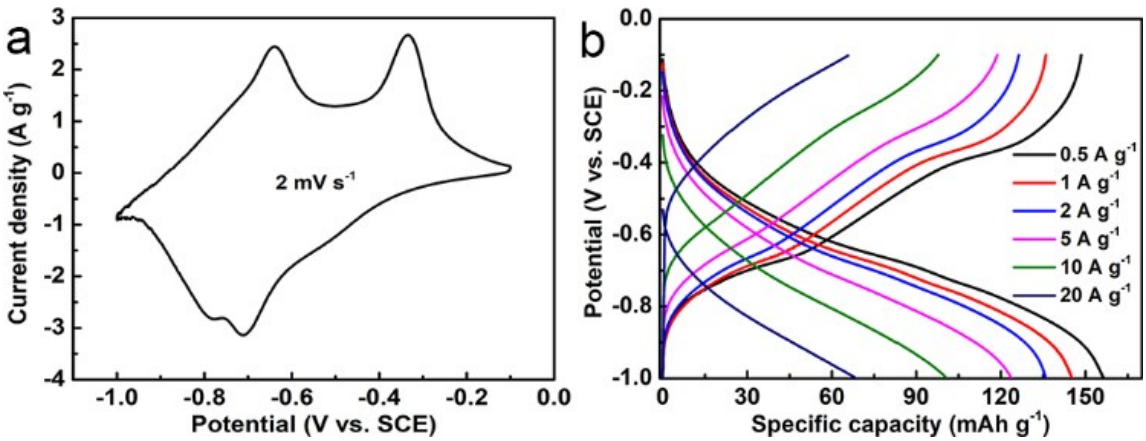

Fig. S9 (a) CV curve of PI and (b) GCD curves of PI at various current densities.

CV curve of PI anode shows two couples of redox peaks (Fig. S9a), corresponding to a two-step reversible enolization. Fig. S9b expresses the GCD curves of PI anode at various current densities. When the current density increases from 0.5 to 20 A g^{-1}, the capacity can retain approximately 44%, illustrating a good rate capability, which may be ascribed to the flexible structure of PI and the small size of hydrated NH_4^+. The results are similar to our previous report.[1]

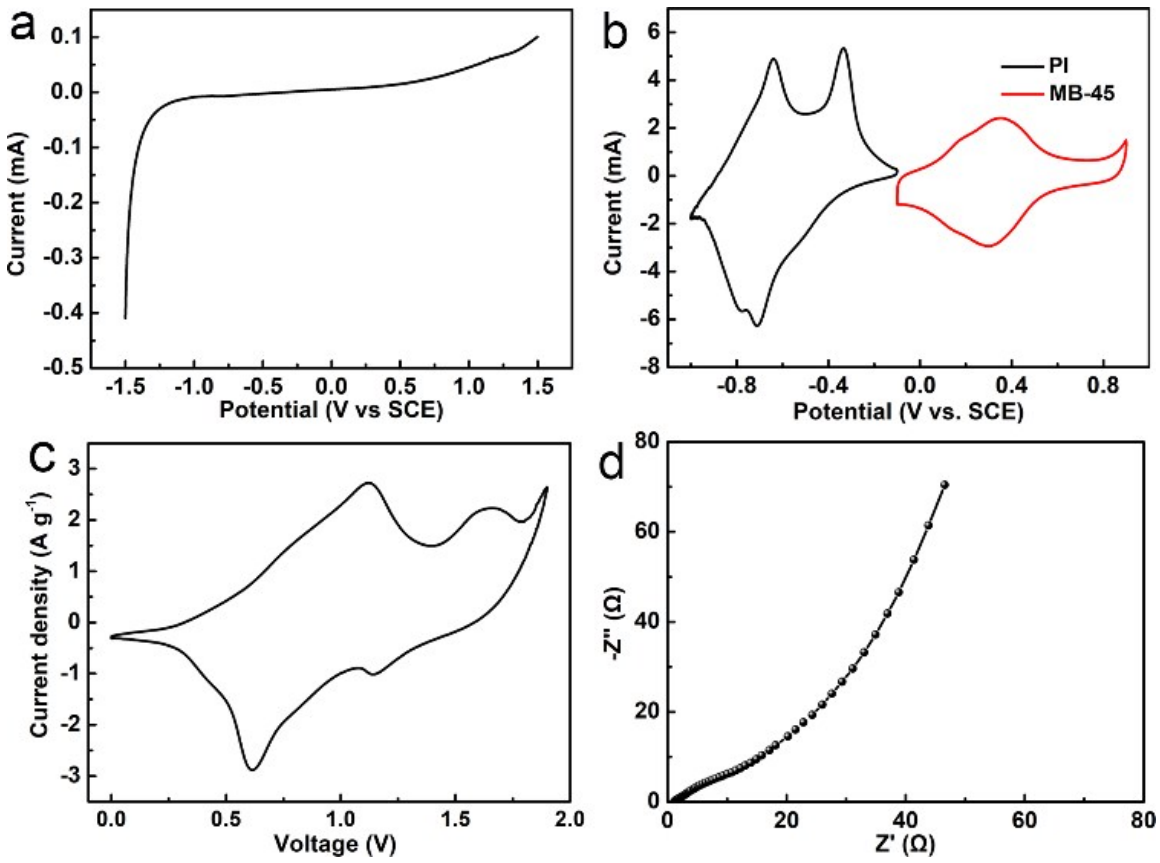

Fig. S10 (a) LSV curve of asymmetric electrolytes based on Ti mesh without active materials, (b) CV curves of PI, MB-45 at 5 mV s^{-1}, (c) CV curve of HIC at a scan rate of 2 mV s^{-1} and (d) Nyquist plots of HIC.

References:

1 Y. Zhang, Y. An, B. Yin, J. Jiang, S. Dong, H. Dou and X. Zhang, J. Mater. Chem. A, 2019, 7, 11314–11320.